LOW-TEMPERATURE
PLASMA

Initiation of High-Voltage Discharge in Air by a Plasma Filament Produced by an Intense Femtosecond Laser Pulse

N. L. Aleksandrov[a], É. M. Bazelian[b], N. A. Bogatov[c], A. M. Kiselev[c], and A. N. Stepanov[c]

[a] *Moscow Institute of Physics and Technology, Institutskiĭ proezd 9, Dolgoprudnyĭ, Moscow oblast, 141700 Russia*
[b] *Krzhizhanovskiĭ Power Engineering Institute, Leninskiĭ pr. 19, Moscow, 117927 Russia*
[c] *Institute of Applied Physics, Russian Academy of Sciences, ul. Ul'yanova 46, Nizhni Novgorod, 603600 Russia*
Received May 5, 2008

Abstract—High-voltage discharge initiated in air by a plasma filament produced by an intense femtosecond laser pulse was studied experimentally. It is found that the threshold of a laser-induced discharge decrease three-fold as compared to that of a discharge in undisturbed air. It is shown that the formation time of a laser-induced discharge decreases by almost three orders of magnitude as the applied voltage increases by a factor of 2. A numerical model of the discharge process is developed that adequately describes the experimental results. In particular, simulations reproduce the experimentally observed steep dependence of the formation time of a laser-induced discharge on the applied voltage, as well as typical values of the electric field required for such a breakdown.

1. INTRODUCTION

Initiation of electric breakdowns in long air gaps by laser pulses have been studied over four past decades [1–19]. These studies are aimed at elaborating methods for controlling the trajectory of a spark discharge, the rate of its development, and the average breakdown field in the discharge gap. In the long-run perspective, the results of these studies can be used to develop megavolt switches and methods for triggering lightnings in thunderstorm clouds. In the past decade, special attention has been paid to filamentary femtosecond laser pulses [10–19]. The filamentation effect is caused by the balance between self-focusing of laser radiation due to the Kerr nonlinearity of air and its defocusing by the plasma produced in the intense field of the self-focused laser beam. In contrast to the bead structure of long laser sparks produced by high-power nanosecond pulses of CO_2 and Nd lasers [4–9], the plasma channel (filament) is continuous and, therefore, is more suitable for using as a conductor that triggers and guides an electric discharge. Experiments have shown that the electron density in the thin (~0.01 cm) plasma channel is about 10^{16} cm^{-3} and the gas temperature is relatively low [20]. The problem of conversion of this channel into a spark is reduced to the analysis of the two possible scenarios: (i) the nonequilibrium laser plasma decays or (ii) the current generated in the channel by a dc voltage applied to the gap has time to heat the gas; slow down electron losses; and, finally, trigger associative ionization reactions involving O and N atoms. Since these reactions can occur without an electric field, the current–voltage characteristic of the discharge

becomes descending, which means completion of spark breakdown. In this respect, the discharge initiated by a laser-produced filament is similar to the streamer discharge of an air gap [21], because, in the latter case, there is also a rapidly forming plasma channel left in air by an ionization wave propagating with a speed of up to 10^9 cm/s. Similar to the filament, the initial gas temperature in the streamer discharge is close to the ambient temperature, while the electron number density can reach 10^{14}–10^{15} cm^{-3}.

The experimental part of this work is aimed at systematic measurements of the characteristics of a high-voltage discharge initiated by a plasma filament. Certain aspects of this problem were studied in earlier publications. For example, laser-spark-aligned localization of a megavolt discharge in a point–plane gap was observed in [15]. It was demonstrated that the velocity of the leader propagating along the laser spark increased tenfold, while the leader threshold halved. A decrease in the threshold of a high-voltage discharge and its localization along the laser beam was also observed in [17]. In [16], a laser-induced discharge was excited in a plane gap to which a dc voltage of a few tens of kilovolts was applied and the dynamics of a low-density channel formed in a gas along the former plasma filament was studied using time-resolved diffractometry. In [16], a model was proposed according to which the reduction in the breakdown voltage of a high-voltage discharge is caused by a decrease in the gas density within the filament due to Joule heating of the plasma by the current generated in the filament under the action of the applied dc voltage.
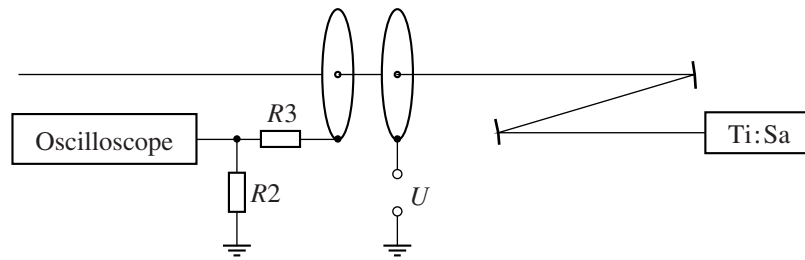
Fig. 1. Scheme of the experiment.

However, many aspects of the influence of a plasma filament created by a femtosecond laser pulse on a high-voltage discharge in a plane gap (which is the easiest to simulate numerically) remain unclear. The main goals of the present study were to measure the breakdown voltage as a function of the laser pulse energy and gap length and investigate the effect of the applied voltage on the time of spark development. The experimental data were used to test the results of numerical simulations of the discharge process with a detailed account of the plasma kinetic processes.

2. EXPERIMENTAL SETUP AND DIAGNOSTIC TECHNIQUES

The scheme of the experiment is shown in Fig. 1. A high dc voltage from a stabilized power source was applied to 60-mm-diameter plane polished duralumin disk electrodes. The interelectrode distance was varied from 1 to 16 mm. The discharge circuit contained a ballast resistance ($R3 = 100\ \Omega$). The current in the discharge circuit was measured using a noninductive shunt ($R2 = 1\ \Omega$) and Tektronix 3052B oscilloscope with a passband of 500 MHz. Laser radiation was input into the discharge gap through 3-mm-diameter rounded-edge apertures at the centers of the electrodes. A femtosecond Ti : Sa laser [22] generated pulses with the wavelength $\lambda \approx 800$ nm, duration $\tau \approx 70$ fs, and energy $W \leq 15$ mJ. The diameter of the output laser beam was 8 mm. Laser radiation was focused by a spherical mirror with a focal length of 80.6 cm. The experiments were performed in atmospheric air.

3. EXPERIMENTAL RESULTS

In the absence of a filament, the breakdown voltage corresponded to the usual breakdown voltage in air [23]. The position of the discharge channel in the electrode plane was random; i.e., the electrode apertures had no effect on the electric strength of the gap. When laser radiation was input to the gap via the electrode apertures, the following was observed. If the energy of the femtosecond laser pulse was insufficient to create a plasma filament, then the gap breakdown voltage remained the same and the position of the discharge channel between the electrodes was random. When the laser pulse energy exceeded the threshold value ($W \approx$ 0.5–0.6 mJ), a plasma channel passing through the electrode apertures and crossing the discharge gap formed in the focal region of the laser beam. In this case, the threshold voltage of a spark discharge decreased significantly and the discharge itself became strictly localized at the place where the filament was produced.

The dependence of the breakdown voltage on the laser pulse energy is shown in Fig. 2. Since the laser energy varied from shot to shot, the following technique was employed to measure this dependence. First of all, the laser was adjusted to generate pulses with a certain average energy. Then, the voltage applied to the electrodes was increased to the level at which the discharge occurred in one-half of the pulses due to fluctuations in the laser pulse energy. The open (closed) cir-
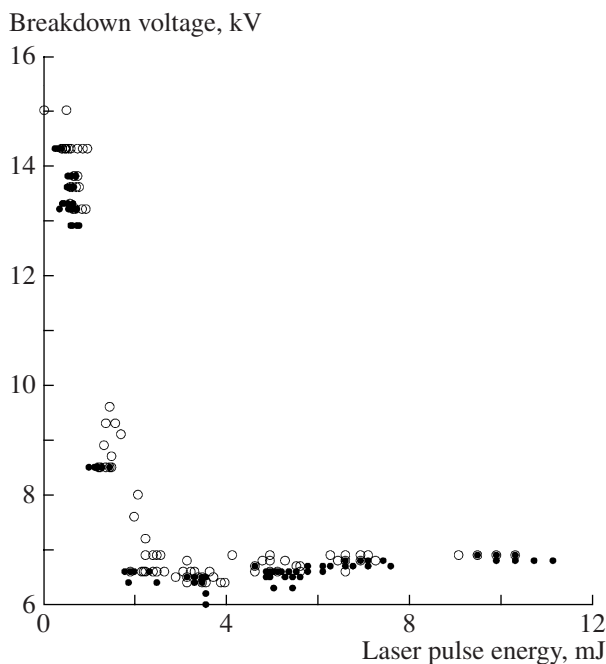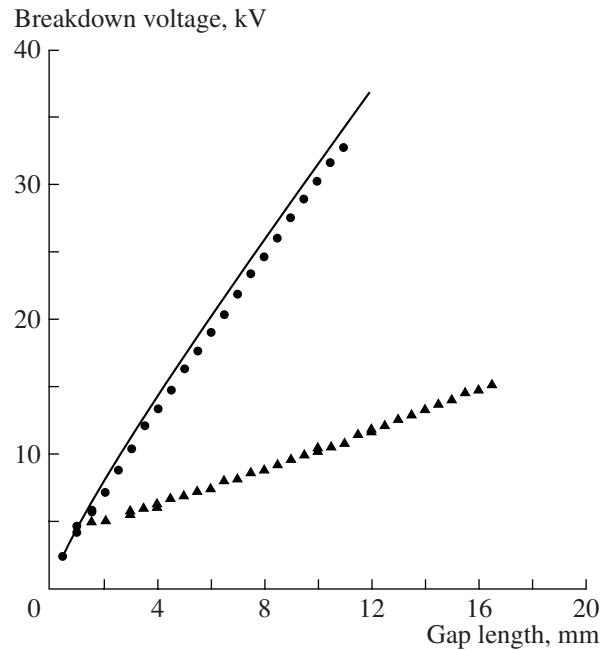

Fig. 2. Breakdown voltage as a function of the laser pulse energy. The open and closed circles correspond to the presence and absence of a discharge, respectively. The distance between the electrodes is $d = 4.5$ mm.

cles in Fig. 2 correspond to the presence (absence) of a breakdown. Then, the procedure was repeated for another averaged laser energy. It is seen from Fig. 2 that, for the gap length $d = 4.5$ mm, the breakdown voltage decreased at least twofold when the filament formed in the gap. As the laser pulse energy increased further, the breakdown voltage remained nearly constant.

Figure 3 shows the measured minimum breakdown voltages U_i and U_{fs} for an undisturbed air gap between plane electrodes in the absence of a filament and for a laser-induced discharge, respectively, as functions of the gap length d. It is seen that, in both cases, the minimum breakdown voltage increases nearly linearly with d. However, for the same gap length, the threshold field in the presence of a filament is much lower, and this difference increases with increasing gap length. Note that the measured values of U_i in an undisturbed air are in good agreement with the data on the breakdown threshold of a plane electrode gap. The data on the breakdown electric field E_{br}, which determines the rate of kinetic processes in the plasma, would be more informative. However, this parameter is difficult to estimate, because the spatial distribution of the applied voltage is rather complicated. In the initial stage of breakdown, just after the formation of the filament, the applied voltage is divided between the filament itself and the two air gaps formed by the filament and the edges of the electrode apertures. The typical lengths of this gaps is about the radius of the electrode aperture, $r_0 \sim 1.5$ mm. As time elapses, the laser-produced plasma is polarized and the field is expelled from the filament to these gaps. Finally, as soon as these gaps are broken, the voltage distribution rearranges again, depending on the conductivities of the filament and the discharge channels formed in the apertures. Taking into account such a complicated sequence of processes, it can be expected that the actual breakdown field E_{br} lies within the interval from $U_{fs}/(d + 2r_0)$ to U_{fs}/d and approaches U_{fs}/d with increasing d. It should be noted, however, that the linear dependence U_{fs}/d indicates that the resistance of the discharge channels formed in the apertures is small and, therefore, E_{br} is closer to U_{fs}/d. This means that, for gap lengths of $d \sim 1$ cm or longer, E_{br} does not exceed 10 kV/cm, which is three times lower than that in an undisturbed air.

The experiments show that the breakdown initiated by a plasma filament is time-delayed with respect to the femtosecond laser pulse. The waveform of the discharge current exhibits two distinct peaks. The first peak corresponds to the above sequence of the processes related to the filament formation by a femtosecond laser pulse, while the second, to the gap breakdown. It is found that the time delay of the breakdown with respect to the laser pulse (the breakdown formation time) depends only slightly on the laser pulse energy. It increases substantially only at energies close to the threshold for filament generation, but decreases

Fig. 3. Breakdown voltages of the self-sustained discharge, U_i (circles), and the discharge initiated by a laser-produced filament, U_{fs} (triangles), as functions of the gap length. The laser pulse energy is $W = 3$–4 mJ. The solid line is the fit of the experimental data on the breakdown threshold for air in a plane gap [20].

significantly with increasing gap voltage (Fig. 4). As the gap voltage increases twofold, this time decreases by almost three orders of magnitude. Such a strong dependence of the breakdown formation time on the applied voltage has never been observed in spark discharges. Observation of such a dependence in numerical simulations could be a fairly strong argument in favor of the validity of the employed numerical model.

4. NUMERICAL SIMULATIONS OF AN AIR GAP BREAKDOWN INITIATED BY A LASER PULSE

The numerical model used in this study does not describe the generation of a filament by a laser pulse and the mechanism of its coupling to the electrodes via the apertures coaxial with the filament. The initial parameters of the model are the electric field, initial electron density, and gas temperature within the filament. The simulations were aimed at describing the plasma dynamics within the filament and the time behavior of the discharge current. Hence, in solving the problem, it was assumed that the electric field in the gap was uniform, the plasma filament contacted the electrodes, and the electric field was established simultaneously over the entire filament length.

In this case, the kinetic scheme of the numerical model does not differ from that used to describe plasma in the streamer channel after it has bridged the gap [21, 24]. The model includes the following balance equa-
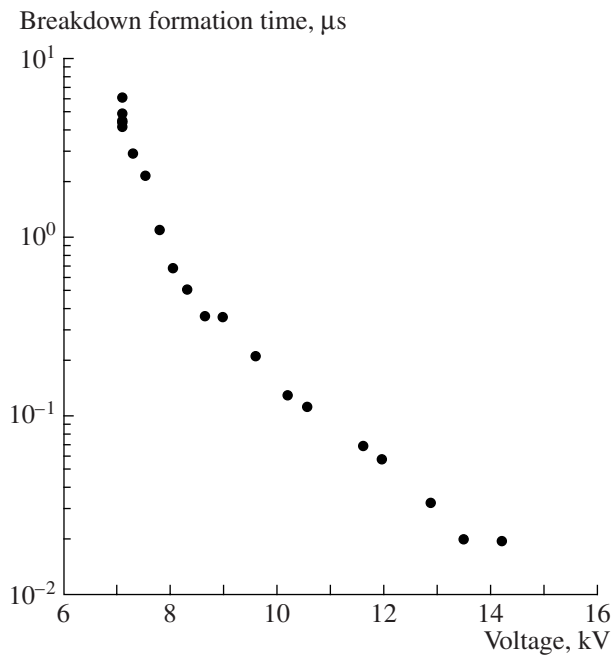
Breakdown formation time, μs

Fig. 4. Breakdown formation time vs. gap voltage for $W = 8–10$ mJ and $d = 4.5$ mm.

tions for electrons, positive and negative ions, and excited and chemically active particles:

$$\frac{\partial n_e}{\partial t} = (k_i N + k_i^* n^*)n_e + k_{ai}N_\text{O}N_\text{N}$$

$$- (k_a' + k_a''N)N_a n_e + (k_d N + k_d^* n^*)n_n - \beta_{ei}n_e n_i, \tag{1}$$

$$\frac{\partial n_p}{\partial t} = (k_i N + k_i^* n^*)n_e$$

$$+ k_{ai}N_\text{O}N_\text{N} - \beta_{ei}n_e n_i - \beta_{ii}n_p n_n, \tag{2}$$

$$\frac{\partial n_n}{\partial t} = (k_a' + k_a''N)N_a n_e - (k_d N + k_d^* n^*)n_n - \beta_{ii}n_p n_n, \tag{3}$$

$$\frac{\partial n^*}{\partial t} = k^* N n_e - k_i^* n^* n_e - k_q^* n^* N. \tag{4}$$

Here, N is the total density of neutral particles; N_a, N_O, N_N, n_e, n_p, n_n, and n^* are the densities of O_2 molecules, O and N atoms, electrons, positive and negative ions, and excited particles, respectively; k_{ai} is the associative ionization rate constant; k_i and k_i^* are the rate constants of direct and stepwise electron-impact ionization; k_a' and k_a'' are the rate constants of dissociative and three-body electron attachment to O_2 molecules; k_d and k_d^* are the rate constants of electron detachment from negative ions due to their collisions with unexcited and excited particles, respectively; k^* and k_q^* are the rate constants of generation and loss of excited particles;

and β_{ei} and β_{ii} are the coefficients of electron–ion and ion–ion recombination. Altogether, the numerical scheme takes into account over 150 reactions involving particles of 27 species.

The gas temperature in the plasma channel was calculated from the equations

$$cN\frac{\partial T}{\partial t} = (\lambda_T + \lambda_R)jE + j_\text{ion}E + Q_{VT}(\varepsilon_v) + Q_{ET}, \tag{5}$$

$$\frac{\partial \varepsilon_v}{\partial t} = \lambda_V jE - Q_{VT}(\varepsilon_v), \tag{6}$$

where λ_T, λ_R, and λ_V are the energy fractions transferred by electrons to molecules due to elastic collisions and excitation of rotational and vibrational levels, respectively; j is the current density in the plasma filament; E is the electric field; j_ion is the ion current density; c is the specific heat of gas per molecule; Q_{VT} is the heat released due to the quenching of the vibrational levels of N_2 molecules in the process of V–T relaxation; Q_{ET} is the heat released due to the fast conversion of the electron energy spent on the excitation of electronic states of molecules [25]; and ε_v is the vibrational energy.

The numerical model implies that the cross section of the plasma channel increases with increasing gas temperature. As a result, the densities of all the plasma components, the reduced field E/N, and, therefore, the rates of electron processes change significantly. Similar to [26], the cross section s of the plasma channel was approximately calculated from the relaxation equation

$$\frac{ds}{dt} = \frac{s_\text{eq} - s}{\tau_s}, \tag{7}$$

where $s_\text{eq}(t) = s_0 T(t)/T_0$ is the asymptotic cross-sectional area corresponding to the current temperature $T(t)$; s_0 and $s(t)$ are the initial and current cross-sectional areas of the channel, respectively; T_0 is the initial temperature; and $\tau_s(t) = r(t)/v_s(t)$ is the current time constant of the relaxation process, which is determined by the current radius $r(t)$ of the channel and the speed of sound $v_s(t)$. The latter depends on the gas temperature $T(t)$ in the channel. This model is valid if the radii of the apertures through which laser radiation is input into the gap are much smaller than the gap length.

Let us first ignore the heating of the plasma filament by the laser pulse and consider the evolution of the plasma parameters under the action of a constant uniform electric field applied to the gap. We assume that the parameters of the filament are constant over its length and radius. The calculations were performed for the following typical parameters [20]: the initial electron density in the filament was $n_{e0} = 3 \times 10^{16}$ cm^{-3}, and its initial radius was $r_0 = 0.005$ cm. The breakdown time was determined from the instant at which the current–voltage characteristics of the plasma channel became descendent. In fact, this occurred when the gas in the channel was heated to 5000 K and the reaction
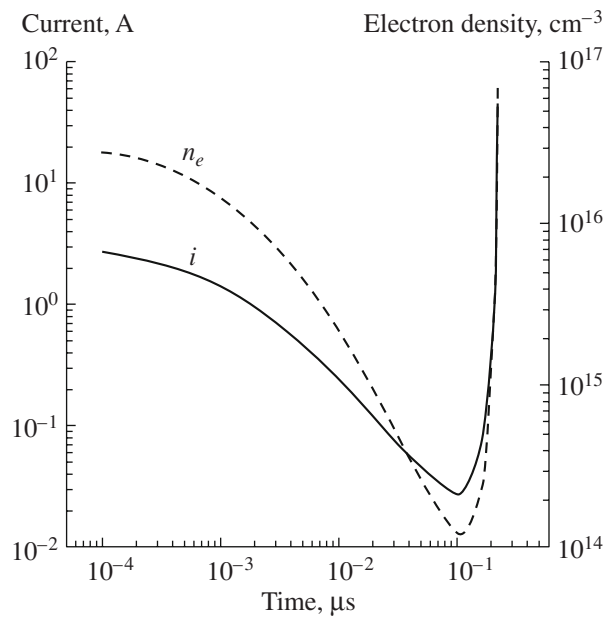
Breakdown formation time, µs
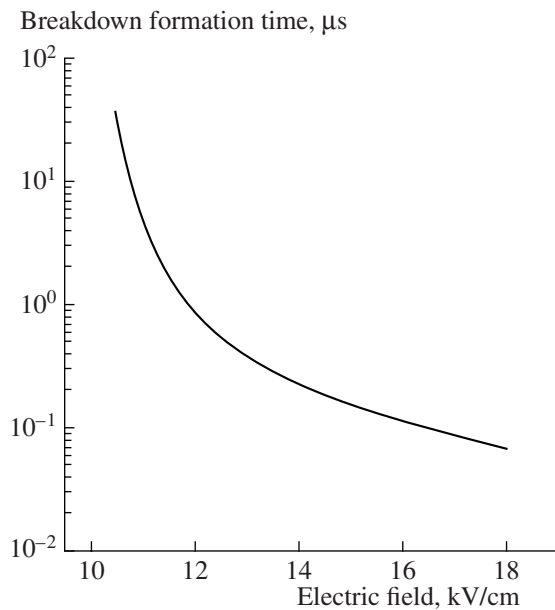
Fig. 5. Calculated time of breakdown formation along a laser-produced filament with a radius of 0.005 cm as a function of the electric field. The initial electron density is 3×10^{16} cm^{-3}.

Fig. 6. Waveforms of the current and electron density in a discharge initiated by a laser-produced filament in an electric field of 14 kV/cm.

$O + N \Rightarrow e + NO^+$ of associative ionization, whose rate is independent of the electric field, became one of the main sources of electrons.

Figure 5 shows the calculated breakdown formation time t_{br} versus the electric field E in the gap. As in the experiment (see Fig. 4), an increase in the electric field leads to a very rapid decrease in t_{br}. This time decreases by two orders of magnitude as E decreases by only a factor of 1.5. An important point is that the simulation results are in good agreement with the experimental data: the minimum and maximum breakdown times are close to 20–70 ns and ~10 µs, respectively. To the best of our knowledge, there is no another form of a spark discharge for which such a slight change in the electric field leads to such a strong variation in the breakdown formation time. In this respect, it is interesting to consider the evolution of the plasma in the course of discharge formation.

The simulation results presented in Fig. 6 were obtained for an electric field in the discharge gap of 14 kV/cm, which corresponds to the breakdown formation time of about 225 ns. Just after the laser pulse, the current flowing along the plasma filament is about 3 A. The current decreases rapidly with time due to intense electron losses in the cold plasma, and the electron density decreases by two orders of magnitude over a time of about 50 ns, the main channel of electron losses during the first 20 ns being electron–ion recombination (over this time interval, the electron density decreases by a factor of 30). Up to the instant of breakdown, the main ion species is O_2^+ (see Fig. 7). The decay of the

plasma filament is accompanied by its continuous heating. The increase in the gas temperature becomes appreciable after about 1 ns, when the temperature increases by about 100 K (see Fig. 8). The temperature increases twofold over 10 ns and threefold over 100 ns. The plasma behavior changes qualitatively at the time of about 115 ns, when the gas temperature increases to 1000 K and the filament cross-sectional area increases by 60%. At this instant, the radius of the expanding channel is 0.00635 cm (Fig. 8) and the reduced field is $E/N \approx 90$ Td (1 Td = 10^{-17} V cm^2). In such a field, the total rate of electron production exceeds their loss rate. As a result, the plasma density begins to increase mainly due to electron-impact ionization of O_2 molecules (Fig. 7). The electron-impact ionization of excited and unexcited N_2 molecules becomes important only 10–20 ns before discharge termination, when E/N becomes higher than 120 Td due to the channel expansion. Associative ionization, $N + O \Rightarrow e + NO^+$, becomes important at temperatures above 5000 K, which are achieved over the last 2 ns before discharge termination.
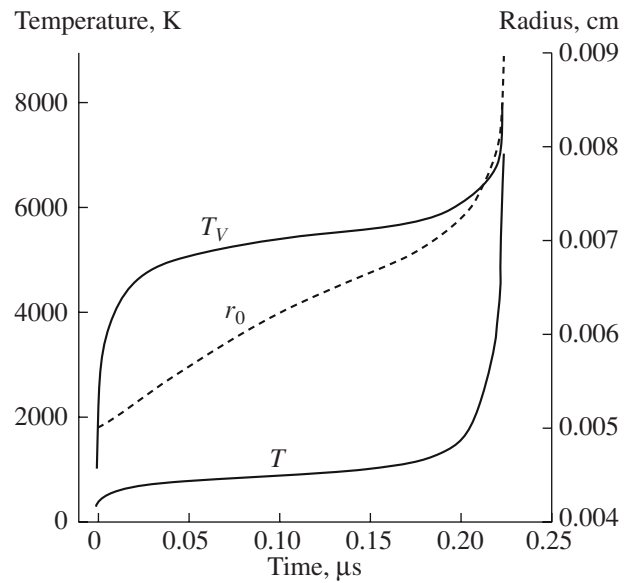
It should be noted that, over a time of about 100 ns, only a minor fraction of the energy stored in the vibrational levels of molecules is spent on the rapid heating of the plasma filament. The most important processes occur at gas temperatures below 1000 K, at which the time constant of V–T relaxation is more than 10 µs even in humid air and reaches 1000 µs in dry air [27]. The decrease in the growth rate of the vibrational temperature (see Fig. 8) also indicates that V–T relaxation plays a minor role.
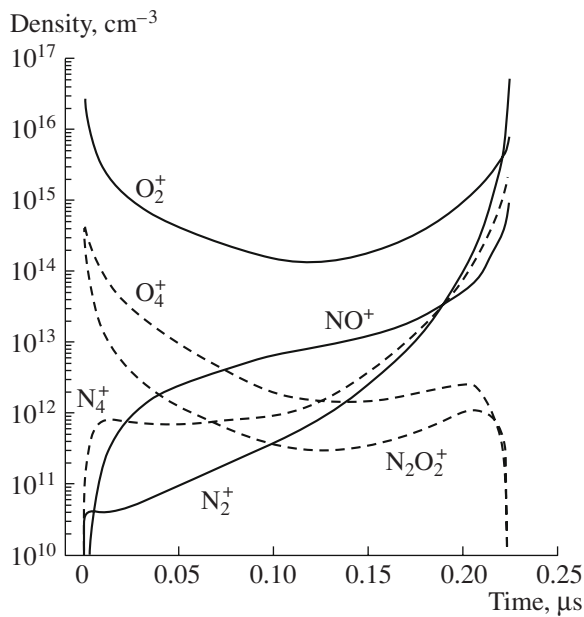
Fig. 7. Dynamics of the ion composition in the discharge plasma under the conditions corresponding to Fig. 6.

Fig. 8. Time dependence of the channel radius and the kinetic and oscillatory gas temperatures under the conditions corresponding to Fig. 6.

The processes remain qualitatively the same also for the slow development of breakdown, when the field applied to the gap is 11.0 kV/cm, which is close to the threshold value. In this case, the plasma stops to decay and, accordingly, the discharge current stops to decrease at the time 1.3 μs. At this instant, the temperature is lower than 550 K, and it becomes higher than 1000 K only 100 ns before breakdown.

Of most interest for practical applications is the minimum electric field at which a laser-induced spark discharge develops in an air gap. According to the experimental data, this field is close to 10 kV/cm. Numerical simulations allow one to find the threshold field as a function of the electron density in the laser-produced filament and the filament radius r_0. The reason why the threshold field depends on the radius is quite evident. A decrease in the radius leads to a proportional decrease in the time constant (see relaxation equation (7)) that determines the rate of filament expansion and increase in the reduced field E/N. Hence, the calculated threshold field should decrease with decreasing r_0. The lower boundary of the dependence $E_{br}(r_0)$ can easily be found by performing numerical simulations at a constant pressure in the channel. In this case, the radius of the filament drops out of the numerical model. The results of simulations are presented in Fig. 9 in the form of the dependence of the breakdown field on the initial electron density n_{e0} in the laser-produced filament. For comparison, the figure also shows the results obtained for $r_0 = 0.005$ cm within the framework of the basic model, which uses relaxation equation (7). It is seen that, as the radius decreases below 0.005 cm, the breakdown field E_{br} decreases insignifi-

cantly. The calculated decrease in the breakdown field is no larger than 10%, while the actual effect will be even less because the model does not takes into account diffusion.
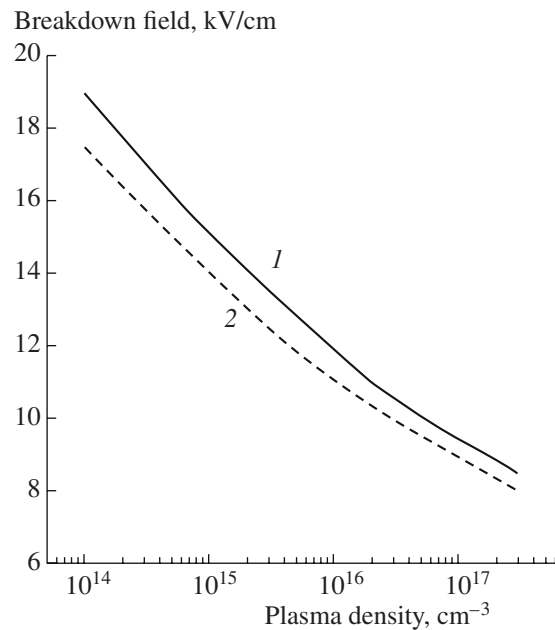
Fig. 9. Calculated breakdown field as a function of the initial electron density in a 0.005-cm-radius laser-produced filament (*1*) for a discharge channel expanding according to the relaxation law and (*2*) at a constant pressure in the channel.

Breakdown field, kV/cm
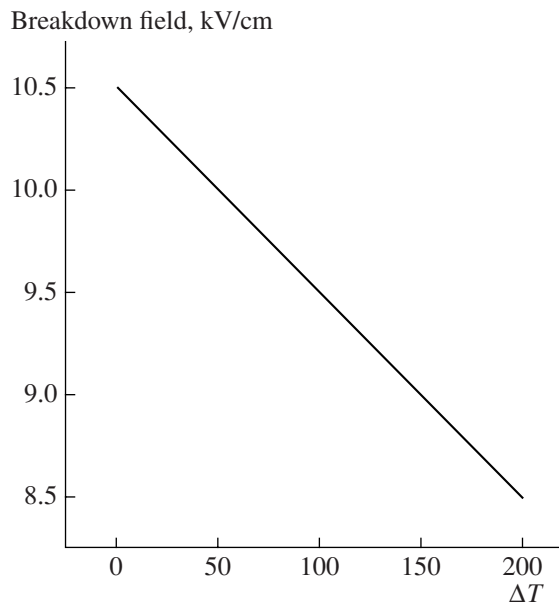
Fig. 10. Breakdown field as a function of the initial gas heating in the laser-produced filament.

The dependence of E_{br} on the initial electron density is more pronounced. It is well known that the typical initial electron density in a streamer under normal conditions is $n_{e0} \approx 10^{14}$ cm^{-3}, which corresponds to $E_{br} \approx$ 19 kV/cm [28, 29]. The same result follows from Fig. 9. As the plasma density increases to values typical of a laser-produced filament ($\sim 10^{17}$ cm^{-3}), the breakdown field halves, which can be important for practical applications.

Finally, it is worth mentioning plasma heating by laser radiation before applying the electric field. According to estimates of the energy spent on gas ionization, the temperature should increase by about 100 K. The numerical data presented in Fig. 10 make it possible to conclude on the effect of such heating. The threshold breakdown field decreases almost linearly to 8.5 kV/cm as the initial increment ΔT in the filament temperature increases to 200 K. Undoubtedly, the decrease in the breakdown field by about 20% is worth studying and should be taken into account in numerical simulations.

5. CONCLUSIONS

The results obtained in this paper can be summarized as follows. Systematic experimental studies have been performed of a high-voltage discharge initiated by a plasma filament in an air gap between plane electrodes—a configuration that is most easy to compare with theoretical calculations.

It is shown that the electric strength of air decreases threefold due to the presence of a nonequilibrium plasma in the filament channel. As the gap voltage increases twofold, the measured breakdown formation time decreases by almost three orders of magnitude. Such a behavior is a specific feature of a spark initiated by a laser-produced filament. Such a strong dependence has never been observed in an undisturbed air.

A numerical model of the discharge process with a detailed account of the plasma kinetic processes and the expansion of the heated filament channel has been developed. The model adequately describes the experimental results. In particular, the simulations reproduce the experimentally observed steep dependence of the breakdown formation time on the applied voltage. The calculated values of the breakdown electric field are close to the measured ones.

REFERENCES

1. A. G. Akhmanov, L. A. Rivlin, and V. S. Shil'dyaev, Pis'ma Zh. Éksp. Teor. Fiz. **8**, 417 (1968) [JETP Lett. **8**, 258 (1968)].

2. L. V. Norinskiĭ, Kvant. Élektron., No. 5, 108 (1971).

3. D. W. Koopman and K. A. Saum, J. Appl. Phys. **44**, 5328 (1973).

4. G. N. Aleksandrov, V. L. Ivanov, and G. D. Kadzov, Zh. Tekh. Fiz. **47**, 2122 (1977) [Sov. Phys. Tech. Phys. **22**, 1233 (1977)].

5. O. B. Danilov and S. A. Tul'skiĭ, Zh. Tekh. Fiz. **48**, 2040 (1978) [Sov. Phys. Tech. Phys. **23**, 1164 (1978)].

6. J. R. Greig, D. W. Koopman, R. F. Fernsler, et al., Phys. Rev. Lett. **41**, 174 (1978).

7. V. D. Zvorykin, F. A. Nikolaev, I. V. Kholin, et al., Fiz. Plazmy **5**, 1140 (1979) [Sov. J. Plasma Phys. **5**, 638 (1979)].

8. M. Miki, Y. Aihara, and T. Shindo, J. Phys. D **26**, 1244 (1993).

9. D. Wang, Z.-I. Kawasaki, K. Matsuura, et al., J. Geophys. Res. **99**, 16 907 (1994).

10. B. La Fontaine, F. Vidal, D. Comtois, et al., IEEE Trans. Plasma Sci. **27**, 688 (1999).

11. S. Tzortzakis, M. A. Franco, Y.-B. André, et al., Phys. Rev. E **60**, R3505 (1999).

12. D. Comtois, C. Y. Chien, A. P. Desparois, et al., J. Appl. Phys. **76**, 819 (2000).

13. B. La Fontaine, D. Comtois, C. Y. Chien, et al., J. Appl. Phys. **88**, 610 (2000).

14. A. Desparois, B. L. Fontaine, A. Bondiou-Clergerie, et al., IEEE Trans. Plasma Sci. **28**, 1755 (2000).

15. H. Pépin, D. Comtois, F. Vidal, et al., Phys. Plasmas **8**, 2532 (2001).

16. S. Tzortzakis, B. Prade, M. Franco, et al., Phys. Rev. E **64**, 57401 (2001).

17. M. Rodriguez, R. Sauerbrey, H. Wille, et al., Opt. Lett. **27**, 772 (2002).

18. R. Ackermann, K. Stelmaszczyk, P. Rohwetter, et al., Appl. Phys. Lett. **85**, 5781 (2004).

19. Y. P. Deng, J. B. Zhu, Z. G. Ji, et al., Opt. Lett. **37**, 546 (2006).

20. F. Theberge, W. Liu, P. T. Simard, et al., Phys. Rev. E **74**, 036406 (2006).

21. N. L. Aleksandrov, É. M. Bazelyan, N. A. Dyatko, and I. V. Kochetov, Fiz. Plazmy **24**, 587 (1998) [Plasma Phys. Rep. **24**, 541 (1998)].

22. A. N. Stepanov, A. A. Babin, A. M. Kiselev, and A. M. Sergeev, Kvant. Élektron. **31**, 623 (2001) [Quant. Electron. **31**, 623 (2001)].

23. *Electrical Breakdown of Gases*, Ed. by J. M. Meek and J. D. Craggs (Wiley, New York, 1978; Inostrannaya Literatura, Moscow, 1980).

24. N. L. Aleksandrov and E. M. Bazelyan, Plasma Sources Sci. Technol. **8**, 285 (1999).

25. N. A. Popov, Fiz. Plazmy **27**, 940 (2001) [Plasma Phys. Rep. **27**, 886 (2001)].

26. E. M. Bazelyan, Yu. P. Raizer, and N. L. Aleksandrov, J. Phys D **40**, 4133 (2007).

27. E. M. Bazelyan and Yu. P. Raizer, *Spark Discharge* (MFTI, Moscow, 1997; CRC, Boca Raton, 1998).

28. A. E. Rodriguez, W. L. Morgan, K. E. Touryan, et al., J. Appl. Phys. **72**, 3957 (1992).

29. N. L. Aleksandrov and E. M. Bazelyan, Fiz. Plazmy **27**, 1121 (2001) [Plasma Phys. Rep. **27**, 1057 (2001)].

Translated by A.V. Serber